

CLUE2GEO: FINE-GRAINED IMAGE GEOLOCATION VIA CLUEMAP AND MULTI-STAGE FINE-TUNING

000
001
002
003
004
005 **Anonymous authors**
006 Paper under double-blind review
007
008
009
010

ABSTRACT

011 Global image geolocation aims to identify the location where an image was cap-
012 tured, but achieving high precision and robust localization remains challenging. To
013 enhance geolocation precision, we present Clue2Geo, a cue-driven framework for
014 global image geolocation, powered by a Large Vision Language Model (LVLM)
015 for coordinate reasoning. Firstly, an LVLM is employed to extract diverse geo-
016 graphic cues from images, after which the reliability and contribution of these cues
017 are assessed by computing their local consistency and semantic coherence. Based
018 on that, a cue graph named “cluemaps” is constructed, which is used as an auxil-
019 iary input both during model fine-tuning and inference. Subsequently, we build a
020 large-scale Street View dataset with coordinates and cluemaps to support a three-
021 stage progressive fine-tuning strategy. This strategy is to enhance the downstream
022 model’s reasoning capabilities for fine-grained localization tasks. Finally, a post-
023 processing refinement based on Retrieval-Augmented Generation (RAG) using a
024 GPS database is applied after reasoning to reduce the offset of the predicted co-
025 ordinates, improving both accuracy and stability. Extensive experiments demon-
026 strate that Clue2Geo achieves state-of-the-art performance on fine-grained met-
027 rics, particularly at the street levels.¹
028

1 INTRODUCTION

029 Global image geolocalization aims to determine the origin of photos taken anywhere on Earth. Com-
030 pared with traditional region-specific methods (Noh et al., 2017; Cao et al., 2020; Lee et al., 2022;
031 Tan et al., 2021; Shao et al., 2023), it offers broader coverage and more diverse applications. How-
032 ever, achieving accurate and robust global localization remains challenging due to significant varia-
033 tions in landscapes, vegetation, buildings, traffic signs across regions, as well as diverse imaging
034 conditions. High-precision tasks, such as street-level localization, are particularly difficult: models
035 must capture fine-grained local features like building details, road signs, landmarks, etc., which vary
036 subtly across regions and are sensitive to viewpoint, lighting, time, and weather. Existing methods
037 often struggle with sparse or noisy local information, and most datasets focus on city- or region-level
038 localization, limiting support for fine-grained, global-scale geolocalization. These factors together
039 constitute the core technical challenge for high-precision global image geolocalization.
040

041 Image geolocalization methods can be broadly categorized into three types: retrieval-based,
042 classification-based, and generation-based. Retrieval-based methods estimate a query image’s lo-
043 cation by comparing it against a database of geo-tagged images and inferring its position from the
044 most similar matches. While intuitive and effective, these methods involve complex feature extrac-
045 tion, high computational costs for nearest-neighbor search, and a strong dependence on the diversity
046 and completeness of the image database. Classification-based methods partition the geographic
047 space into discrete regions and assign images to the corresponding region. This approach can-
048 not achieve coordinate-level fine-grained localization; the region partitions often fail to reflect true
049 geographic distributions, and the models generally operate as black boxes, lacking interpretable rea-
050 soning. Generation-based methods treat geolocalization as a GPS coordinate generation task, using
051 large models to directly predict image coordinates. Although effective on coarse-grained bench-
052 marks, their performance is limited by model knowledge and the inherent randomness of outputs,
053 making high-precision localization challenging.

¹Our code and dataset is available at <https://github.com/xxxxxx>

We propose Clue2Geo, a globally oriented image geolocation framework driven by structured cues, to address the limitations of existing methods. Explicitly extracting and structuring cues can direct models' attention to key features and their relationships. Therefore, geographic cues such as landmarks are extracted from images using an LVLM and organized into a structured cue graph named "cluemaps" as an auxiliary input during fine-tuning and inference. Then, an LVLM is employed to predict the coordinates where images were captured. To enhance the model's fine-grained geolocation and reasoning capabilities, a three-stage fine-tuning strategy is applied, using data that integrates cluemaps with the reasoning process to progressively fine-tune the model at different geographic scales and improve its overall performance. Finally, to mitigate the inherent uncertainty, particularly the coordinate deviations in fine-grained localization, a RAG-based post-processing module proposed in prior studies (Zhou et al., 2024; Jia et al., 2024; Vivanco Cepeda et al., 2023) is incorporated. By referencing large-scale image-coordinate pairs to enhance generation, this module refines the final predicted coordinates, significantly enhancing both robustness and accuracy while demonstrating strong generalization capability. We summarize the main contributions of our work as follows:

- We propose Clue2Geo, a framework for global image geolocation that leverages an LVLM to predict coordinates. The LVLM is progressively fine-tuned in stages using structured cues to enhance reasoning and fine-grained localization, and final coordinate is chosen by matching encodings of the fine-tuned LVLM and RAG predictions with image encoding.
- A method for constructing a cluemaps is proposed, in which high-value cues are identified by computing their local consistency and semantic cohesion, and other cues are linked to them based on semantic similarity. The cluemaps guides LVLM to prioritize informative cues and enhances its ability to understand and reason over complex geographic information.
- A large-scale Mapillary-based dataset containing coordinates, addresses, and visual cues was built and employed for fine-tuning, through which the LVLM's reasoning capabilities and its utilization of complex geographic cues are significantly enhanced.
- Extensive experiments are conducted on two public datasets, IM2GPS3K and YFCC4K. The results demonstrate that Clue2Geo consistently outperforms state-of-the-art baselines in fine-grained localization.

2 RELATED WORK

Image geolocalization Image geolocalization has received increasing attention in recent years, with applications spanning navigation, urban planning, criminal investigation, and multimedia retrieval. Existing approaches can be broadly categorized into three types: retrieval-based, classification-based, and generation-based methods. Retrieval-based methods estimate the location of a query image by comparing it against a database of geotagged images and inferring its position from the most similar matches (Regmi & Shah, 2019; Shi et al., 2019; 2020; Toker et al., 2021; Zhu et al., 2022; 2021; Workman et al., 2015; Liu & Li, 2019). Vivanco Cepeda et al. (2023) proposed an image-to-GPS retrieval method that explicitly aligns image features with corresponding GPS coordinates to tackle global geolocalization. However, these methods require building and maintaining a reference database, which remains impractical at large scales. To overcome this limitation, Weyand et al. (2016) proposed dividing the Earth into discrete geographic categories for image location prediction. By constructing these categories, predictions can be made at either coarse or fine granularity based on the spatial extent of each category. Nonetheless, classification-based methods (Seo et al., 2018; Vo et al., 2017; Muller-Budack et al., 2018; Pramanick et al., 2022; Clark et al., 2023; Izbicki et al., 2019) often represent each category by its centroid coordinates. Even when a category is correctly predicted, significant errors may occur if the actual image location is distant from the category center. With the rapid development of generative models, generation-based methods have gradually emerged. Zhou et al. (2024) introduced retrieval-augmented generation (RAG) into geolocalization, using coordinates of similar images as references to assist large language models (LLMs) in predicting locations. Building on this, Jia et al. (2024) integrated geographic information into image representations and leveraged geographic diversification and verification to improve prediction performance and robustness. Li et al. (2024) employed LVLMs along with external knowledge from human reasoning to perform geolocalization on street-level imagery. Dufour et al. (2025) applied diffusion models to image geolocalization by treating coordinates as continuous spatial points: they

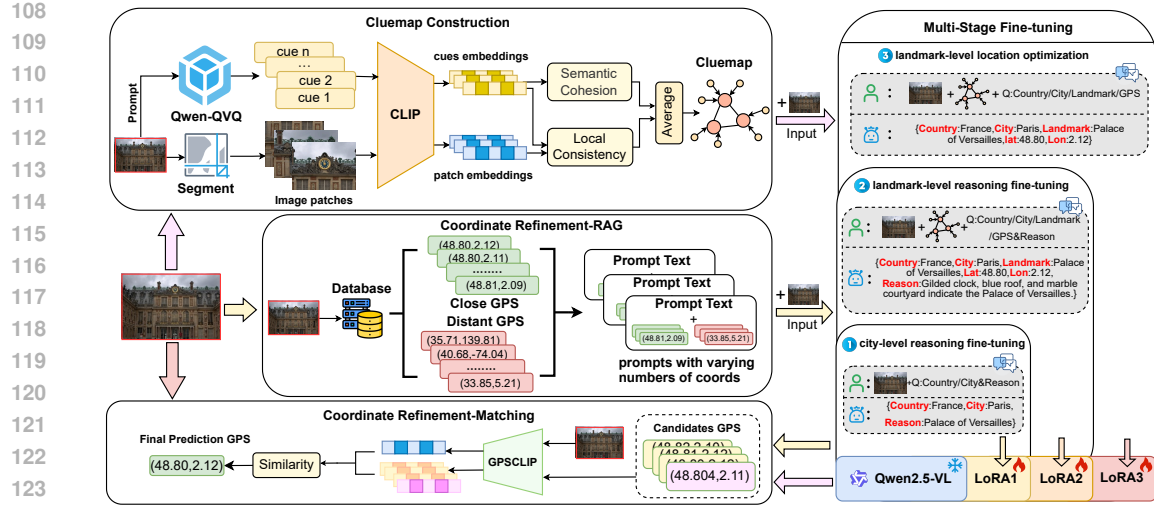


Figure 1: The overall framework of Clue2Geo consists Multi-Stage Fine-tuning, Cluemap Construction, and Coordinate Refinement. A reasoning model is first obtained via three-stage LoRA fine-tuning on Mapillary dataset. Cluemap Construction extracts cues and segments the image, encoding textual cues and patches with CLIP to build a Cluemap as one input, while Coordinate Refinement-RAG retrieves reference coordinates to form another input. At inference, the model processes these two inputs separately to produce candidate coordinates, and the Matching stage uses GPSCLIP to select the final coordinate.

progressively added noise to true coordinates and trained a network to predict the noise conditioned on images, thereby learning the correspondence between visual content and geographic locations.

Large Multimodal Models Inspired by the success of large models in single domains, researchers have increasingly focused on cross-modal large models. CLIP(Radford et al., 2021) aligns image and text representations via contrastive learning, achieving strong cross-modal generalization with a simple objective. Building on this, LLAVA(Liu et al., 2023) combines CLIP’s visual encoder with the Vicuna language model and employs a two-stage instruction fine-tuning strategy to enhance performance in vision-and-language understanding. In 2023, OpenAI released the multimodal GPT-4V(Achiam et al., 2023), capable of processing both text and image inputs to generate responses, further demonstrating the potential of multimodal models for unified understanding and reasoning tasks. These models not only grasp cross-modal semantics but also exhibit strong capabilities in complex reasoning and generation. Recently, numerous high-performing multimodal models have emerged globally(Jia et al., 2018; 2023; Li et al., 2023). The Qwen-VL(Bai et al., 2023; 2025; Wang et al., 2024) series, as a representative open-source model, combines powerful visual encoding and language understanding, leveraging large-scale image-text pretraining and instruction fine-tuning to achieve superior performance in image-text alignment, cross-modal question answering, and visual reasoning, providing strong support for research in computer vision(Wang et al., 2023), natural language processing(Zhao et al., 2023), and multimodal learning(Yin et al., 2024).

3 METHOD

Figure 1 illustrates the overall architecture of Clue2Geo. It contains three components:cluemap construction for extracting and modeling visual cues, three-stage localization fine-tuning to enhance geographic reasoning, and a post-coordinate refinement module to improve predicted coordinates via RAG. The fine-tuning dataset was described at the end.

3.1 CLUEMAP CONSTRUCTION

Visual Cue Extraction Conventional image geolocation that relies solely on pure image inputs often fails to capture the most distinctive local details essential for fine-grained localization. By explicitly extracting visual cues from images and evaluating their localization value, then combining them

with the original image, the model can focus on the most distinctive and informative regions while retaining overall context, significantly outperforming pure image input in fine-grained localization tasks. Therefore, we first extract geography-related cues from images using Qwen-QVQ. A structured prompt is designed that enumerates seven representative categories of geographically relevant cues, including landmark buildings, natural landscapes, scene types, recognizable text, vehicle characteristics, typical clothing or activities, and overall environmental context. This categorization in the prompt is not a restriction but rather guidance, helping the model form a clearer sense of direction when extracting information. At the same time, the prompt explicitly encourages the model to go beyond these seven categories and capture any additional cues that may aid geolocation, thereby ensuring comprehensive and fine-grained cue collection.

However, the existing reasoning of LVLM is not strictly deductive reasoning, but rather relies on statistical rules, semantic similarity, and retrieval-based memory to "simulate" reasoning, by verifying candidate answers rather than deduction. This verifier-style reasoning can cause cascading errors, where an incorrect initial answer leads all subsequent steps to follow and reinforce the same mistake. Thus, to prevent errors during the extraction stage that could propagate into comprehensive mistakes in subsequent reasoning, the content of the cues is strictly constrained. Specifically, the cues are limited to listing all visually identifiable elements potentially related to geographic location, without making any form of location prediction. In other words, the goal of this step is to maximize the fidelity and completeness of the information rather than directly infer coordinates, thereby providing a reliable, objective, and interpretable input foundation for subsequent geolocation reasoning. The formalization of cue extraction is as follows:

$$C = \{c_1, c_2, \dots, c_n\} = f_{\text{extract}}(p) \quad (1)$$

f represents an LVLM. Given an input prompt p , f extracts a structured set of visual cues C potentially relevant to geographic location, strictly avoiding any form of location prediction. The content of the prompt p can be found in the appendix A.1.1.

Cluemap Construction It is worth noting that, due to hallucinations, the cues extracted by LVLM are not always accurate and do not always contribute to geolocation. To assess which cues are accurate and contribute meaningfully, we introduce local consistency and semantic coherence.

Local consistency measures whether the content described by cues is supported by the visual information in the image, that is, whether the cues are accurate and reliable. Since cues often describe local regions of an image, directly computing similarity between a cue and the entire image may not accurately reflect its correctness. We propose two methods of varying complexity to calculate local consistency. Scheme 1 involves performing semantic segmentation on the image, identifying the objects corresponding to the cues, and computing the similarity between them as the local consistency. Scheme 2 divides the image into fixed-size patches, calculates the similarity between the cues and each patch, and takes the maximum value as the local consistency. Since constructing a cluemap for 70,000 images during subsequent fine-tuning would make semantic segmentation computationally expensive and time-consuming, we adopt the simpler Scheme 2 to approximate the local consistency of the cues. The cues and patches are encoded separately using CLIP's (Radford et al., 2021) text and visual encoders, and the cosine similarity is subsequently calculated. The calculation process of local consistency is as follows:

$$S_l(c, I) = \max_{j \in \{1, \dots, M\}} \text{sim}(c, I_j) \quad (2)$$

Here, c denotes a specific extracted cue, I represents the entire image, and I_j denotes the j -th image patch after dividing the image into M patches. The function $\text{sim}()$ is cosine similarity. The local consistency score S_l of cue c with respect to image I is determined by the maximum similarity between the cue and all patches.

Semantic coherence is defined as measuring the strength of a cue's relationships with other cues, capturing its semantic connectedness within the overall cue set. When multiple cues describe the same object, their coherence scores tend to be higher, which often indicates richer visual elements, and thus potentially greater contribution to geolocation. However, low-coherence "isolated cues" are not assumed to be unimportant; we acknowledge that such cues may still play a critical role. In this work, we retain all cues to form a complete cluemap structure but use semantic coherence solely to describe the strength of relationships without assigning additional weights or special treatment to isolated cues. We employ Sentence-BERT to encode the cues and calculate their pairwise cosine similarity. The calculation of semantic coherence is formulated as follows:

216
217
218
219
220

$$S_s(c_i, C) = \frac{1}{|C| - 1} \sum_{\substack{j=1 \\ j \neq i}}^{|C|} sim(c_i, c_j) \quad (3)$$

221 Let $C = \{c_1, c_2, \dots, c_{|C|}\}$ denote the set of all cues, where $c_i \in C$ represents the i -th cue. The
222 function $sim(c_i, c_j)$ measures the cosine similarity between cue c_i and cue c_j . The semantic co-
223 herence score $S_s(c_i, C)$ of cue c_i is computed as the average semantic similarity between c_i and all
224 other cues in C .

225 In order to balance both the reliability and the contribution of each cue, the two scores are jointly
226 considered to provide a comprehensive assessment of cue value. Specifically, an equally weighted
227 (0.5 each) average is employed to derive the final relationship strength, which captures not only
228 the semantic connections between a cue and the other cues but also the alignment between the cue
229 description and the actual image. The calculation of relationship strength S_r is formulated as follows:

$$S_r(c_i) = \alpha S_l(c_i) + (1 - \alpha) S_s(c_i), \quad \text{with } \alpha = 0.5 \quad (4)$$

232 Finally, based on the final relationship strength, the three highest-scoring cues are selected as pri-
233 mary nodes. The remaining cues are attached to the corresponding primary nodes according to their
234 semantic similarity, thereby forming a graph structure termed Cluemap. In this structure, being a pri-
235 mary node indicates that the cue has comparatively higher and more reliable localization value, while
236 its associated neighboring cues provide complementary information to that primary node. In other
237 words, all cues are organized into three clusters centered on the primary cues, offering a structured
238 representation of the image cues. The constructed Cluemap is subsequently used as supplementary
239 information during fine-tuning and inference to enhance geolocation accuracy.

240

241 3.2 MULTI-STAGE LOCALIZATION FINE-TUNING

242

243 Although LVLMs show strong generalization ability, they struggle with fine-grained geolocation
244 due to insufficient optimization for subtle, domain-specific cues. Fine-tuning on curated data with
245 explicit geographic information adapts the model to these nuances, improving accuracy and inter-
246 pretability. More importantly, studies have demonstrated that integrating the reasoning process can
247 enhance the capabilities of LLMs (Qiao et al., 2022). Therefore, fine-tuning the model with a focus
248 on reasoning substantially improves its performance in geolocation tasks.

249

250 Because geolocation involves hierarchical information ranging from city-level to landmark-level, a
251 single-stage approach is often insufficient. Therefore, we adopt a three-stage fine-tuning strategy:
252 first performing reasoning-oriented fine-tuning at the city and landmark levels, and then conducting
253 location-optimization fine-tuning at the landmark level. This coarse-to-fine adaptation progressively
254 improves the model’s reasoning ability and accuracy. Qwen2.5-VL-7B is adopted as the base model
255 for fine-tuning in our framework.

256

257 To enhance the model’s reasoning capability at the city level, coarse-grained city-level reasoning
258 fine-tuning is first conducted. In this stage, the fine-tuning inputs contain only simple cue reasoning,
259 aiming to train the model to acquire a foundational pattern of coarse-grained geospatial reasoning.
An example data template for this stage is shown below (format only; detailed content is provided
in the Appendix A.1.2):

260

[Input]: {Image:Image, Question:Which country and city is the image located in?Explain reason.}
[Output]: {Country:“France”,City:“Paris”,Reason:“French text and the Eiffel Tower.”}

262

263 After the model had initially acquired a basic understanding of geographic reasoning, fine-grained
264 landmark-level reasoning fine-tuning is conducted. In the fine-tuning data, the model was explicitly
265 provided with structured cues and was guided to perform step-by-step reasoning, further enhancing
266 its sensitivity to geographic visual cues at the landmark level and its ability to reason from such cues.

267

268 The fine-tuning data was built by first constructing cluemaps using the method described in Section
269 3.1. Geographic visual cues were extracted from images and structured alongside the original images
to form multimodal inputs, enabling the model to access both visual information and structured geo-
graphic cues. Step-by-step reasoning chains were then generated for each sample using an LLM,

followed by manual review and refinement to ensure the accuracy and logical consistency of the reasoning process. Finally, the image, cluemap, validated reasoning chain, true location, and coordinates were integrated into a complete training instance, and the prompt was designed to explicitly instruct the model to reference the cluemap when reasoning, thereby creating a mapping from visual cues to geographic coordinates. The fine-tuning data template for this stage is as follows:

[Input]: {Image:Image, Question: Predict the location from the image and clues:ClueMap.Explain reason. }
[Output]: {Country:“France”,City:“Paris”,Landmark:“Eiffel Tower”,lat:48.8584,lon:2.2945,
Reason:“French text and the Eiffel Tower.”}

In real world geolocation applications, most use cases require only the final coordinate and address rather than a reasoning chain. Therefore, in the final landmark-level location optimization stage, we remove the reasoning outputs and train the model to directly predict precise coordinates and addresses. This design encourages the model to internalize the reasoning process it acquired in the earlier stages and focus on end-to-end geolocation accuracy. The input format from the second stage was retained, with both the original image and the structured cluemap provided so that geographic cues and semantic associations could still be fully leveraged by the model during inference. However, reasoning chains were no longer supplied; instead, the model received the inputs and directly produced the final predicted location and coordinates. This approach strengthened its end-to-end geolocation capability, enabling it to continually align with the real world geographic distribution during training and gradually establish a stable mapping from visual cues to precise coordinates. The fine-tuning data template for this stage is as follows:

[Input]: {Image:Image, Question: Predict the location from the image and clues: ClueMap.explain reason. }
[Output]: {Country: "France", City: "Paris", Landmark: "Eiffel Tower", lat:48.8584,lon:2.2945}

3.3 POST-PROCESSING COORDINATE REFINEMENT

Because of the inherent randomness in LLM outputs, predicted coordinates can inevitably deviate, and repeated predictions for the same image may vary, undermining both stability and accuracy. To address this, we adapt the RAG module proposed in (Jia et al., 2024) as a post-processing step for Clue2Geo, leveraging a retrieval database with large-scale image–coordinate mapping to more precisely align predicted results with real geographic locations and thereby enhance fine-grained geolocation accuracy and robustness. By providing a set of retrieved ‘anchor’ coordinates, the generative space is constrained to more reliable regions and prediction drift is mitigated. Both the model’s direct predictions and the retrieval-augmented outputs are leveraged and compared with the image embeddings to identify the closest match. This process effectively yields multiple independent estimates and chooses the most consistent one, which from a statistical perspective reduces variance and leads to more stable and accurate geolocation results.

The retrieval database consists of a large set of known image–coordinate pairs, with images aligned to coordinates using a pre-trained CLIP model proposed in (Jia et al., 2024)(hereinafter referred to as GPSCLIP). Each image is represented as a high-dimensional feature vector capturing both visual and latent geographic information. The input image is encoded and matched against the database samples based on feature similarity, selecting the most and least similar coordinates as reference. Multiple prompts are constructed based on the number of reference coordinates to separately guide the model’s outputs. The outputs, together with the direct output from the fine-tuning stage , are encoded using GPSCLIP, and their similarity to the image embeddings is computed to identify the most similar coordinates as the final prediction. This approach effectively reduces prediction bias and enhances stability and accuracy in fine-grained localization at both city and landmark levels.

3.4 MAPILLARY DATASET

We collected 70,000 high-quality street-view images along with corresponding metadata from multiple popular cities worldwide using the open street-view platform Mapillary. Leveraging the latitude and longitude information in the metadata and utilizing Here Maps' reverse geocoding service, we geographically annotated each image and organized locations into three hierarchical levels: country, city, and landmark. Additionally, following the cue extraction method proposed in Section 3.1, we extracted at least five visual cues from each image to support subsequent image-based geolocation reasoning and localization studies.

Table 1: Comparison of Clue2Geo with Other Models on the Im2GPS3k and YFCC4K Dataset.

Dataset	Method	Street(1km)	City(25km)	Region(200km)	Country(750km)	Continent(2500km)
Im2GPS3k	[L]kNN, $\sigma = 4$	7.2	19.4	26.9	38.9	55.9
	PlaNet	8.5	24.8	34.3	48.4	64.6
	CPlaNet	10.2	26.5	34.6	48.6	64.6
	ISNs	10.5	28.0	36.6	49.7	66.0
	TransLocator	11.8	31.1	46.7	58.9	80.1
	GeoDecoder	12.8	33.5	45.9	61.0	76.1
	G3	14.55	37.80	52.95	70.30	83.52
	GeoCLIP	13.31	32.47	48.28	66.67	82.65
	PIGEON	11.3	36.7	53.8	72.4	85.3
	Plonk	6.17	37.17	51.28	67.00	81.85
	Clue2Geo	18.55	41.98	55.56	70.87	84.22
YFCC4K	[L]kNN, $\sigma = 4$	2.3	5.7	11	23.5	42
	PlaNet	5.6	14.3	22.2	36.4	55.8
	CPlaNet	7.9	14.8	21.9	36.4	55.5
	ISNs	6.5	16.2	23.8	37.4	55
	TransLocator	8.4	18.6	27.0	41.1	60.4
	GeoDecoder	10.3	24.4	33.9	50.0	68.7
	G3	23.10	33.49	44.49	61.66	76.61
	GeoCLIP	9.59	19.29	32.61	54.98	74.67
	PIGEON	10.4	23.7	40.6	62.2	77.7
	Plonk	6.5	32.05	43.69	59.35	75.24
	Clue2Geo	23.39	33.77	44.66	62.46	77.78

4 EXPERIMENTS

4.1 EVALUATION DETAILS

The model was fine-tuned according to the strategy described in Section 3.2. Its performance was then evaluated on the public datasets Im2GPS3k (Vo et al., 2017) and YFCC4k (Vo et al., 2017), with all LLM-based methods standardized by replacing their base models with Qwen2.5-VL-7B to eliminate differences arising from model architectures. For each test image, we computed the great-circle distance between the predicted and ground-truth coordinates and quantified the proportion of predictions falling within distance thresholds of 1 km, 25 km, 200 km, 750 km, and 2500 km.

4.2 COMPARISON WITH STATE-OF-THE-ART METHODS

To validate the effectiveness of Clue2Geo, we conducted comparative experiments against other state-of-the-art methods on the IM2GPS3K and YFCC4K datasets. Tables 1 present the performance comparison of Clue2Geo with other methods. GeoReasoner (Li et al., 2024) is not included in our comparison, as its results could not be reproduced with the provided weights, its fine-tuning data is unavailable, and the reported metrics were incomplete.

Our approach achieved state-of-the-art performance in fine-grained (street-level) geolocation tasks on both the Im2GPS3K and YFCC4K datasets, while remaining competitive at broader geographic scales. On Im2GPS3K, our method reached 18.55%, 41.98%, and 55.56% within the 1 km, 25 km, and 200 km thresholds, respectively—improving over the second-best method by 4.0%, 4.2%, and 2.6%, with especially notable gains at street and city scales. On YFCC4K, our method achieved 23.39%, 33.77%, and 44.66% on the 1 km, 25 km, and 200 km fine-grained metrics, matching or slightly surpassing the best-performing method (G3) with gains of 0.29%, 0.28%, and 0.17%, while maintaining nearly identical performance on the 750 km and 2500 km coarse-grained metrics (differences of only 0.2–0.4%). These results demonstrate that our approach advances high-precision, fine-grained geolocation without sacrificing accuracy at coarser scales (national/continental level), achieving a stronger balance and greater robustness in multi-scale geolocation tasks.

378

379

Table 2: The ablation results of Clue2Geo on Im2GPS3k (with Coordinate Refinement).

380

Method	Street(1km)	City(25km)	Region(200km)	Country(750km)	Continent(2500km)
w/o RC	18.02	41.64	55.39	70.77	84.05
w/o RL	16.35	40.71	54.21	70.20	83.88
w/o OL	15.54	38.07	52.65	69.67	83.52
w/o CM	17.78	40.57	54.02	69.36	83.38
w/o CR	15.45	41.04	55.26	70.47	83.92
Clue2Geo	18.55	41.98	55.56	70.87	84.22

388

389

390 Clue2Geo achieves state-of-the-art performance in geolocation prediction, though its effectiveness
 391 varies across different datasets. On the IM2GPS3k dataset, our approach significantly outperforms
 392 existing models, primarily because the dataset was originally designed for geolocation tasks. Its
 393 carefully curated, high-quality images contain rich visual cues that align closely with the Street
 394 View images used for fine-tuning. Street View provides abundant and consistent geographic signals,
 395 such as architectural styles and road layouts, enabling the model to effectively learn and transfer
 396 fine-grained spatial patterns. In contrast, the YFCC4k dataset, sourced from Flickr, consists of di-
 397 verse and noisy user-uploaded images. Variations in image quality, camera angles, and lighting
 398 conditions, combined with inaccurate location tags and a scarcity of useful geographic cues, create a
 399 pronounced domain shift. This limits the model’s ability to extract generalizable features, resulting
 400 in less pronounced performance gains compared to IM2GPS3k. Despite these challenges, Clue2Geo
 401 demonstrates strong performance on both datasets, highlighting its robust generalization ability and
 402 effectiveness in handling diverse and noisy data.

402

403 Clue2Geo demonstrates significant advantages in fine-grained geolocation tasks, primarily due to
 404 high-fidelity cue modeling and multi-stage fine-tuning. By extracting and structurally organizing
 405 geographic cues from images, it constructs a cluemap that is both semantically consistent and lo-
 406 cally sensitive, enhancing the model’s discriminative ability in dense visual feature spaces. The
 407 multi-stage fine-tuning strategy strengthens representation transfer from coarse to fine granularity,
 408 improving discriminability and robustness at the city and landmark levels, while coordinate refine-
 409 ment leverages real-world geographic distributions to further reduce prediction errors. Through
 410 the synergy of these mechanisms, Clue2Geo achieves substantial performance gains over baseline
 411 models at fine-grained thresholds, while maintaining superior generalization and interpretability.

411

412

4.3 ABLATION STUDY

413

414 We performed ablation experiments on IM2GPS3K to evaluate our methods.

415

- 416 • w/o RC: Remove the city-level reasoning fine-tuning stage.
- 417 • w/o RL: Remove the landmark-level reasoning fine-tuning stage.
- 418 • w/o OL: Remove the landmark-level location optimization stage.
- 419 • w/o CM: Omit the ClueMap and feed only the raw images.
- 420 • w/o CR: Remove the post-coordinate refinement.

421

422 Table 2 presents the ablation results on Im2GPS3k. When any individual module is removed, per-
 423 formance drops to varying degrees, and these declines closely match the expected roles of each module.
 424 Removing RC lowers Street, City, and Region to 18.02%, 41.64%, and 55.39%, respectively, with
 425 the largest drops at street and city levels, confirming its role in building spatial layout awareness and
 426 providing a stable foundation for finer-grained reasoning. Removing RL reduces Street accuracy to
 427 16.35% and City to 40.71%, showing that the model’s fine-grained reasoning capacity is weakened,
 428 underscoring the importance of cues and reasoning processes introduced at this stage for strengthen-
 429 ing multi-level reasoning. Removing OL produces the steepest performance drop, with Street, City,
 430 and Region metrics falling to 15.54%, 38.07%, and 52.65%, respectively, demonstrating that this
 431 module is indispensable for enhancing the model’s direct fine-grained location prediction capability;
 432 by training intuitive localization beyond reasoning, it preserves both high accuracy and high capac-
 433 ity in multi-scale tasks. Removing CM lowers Street, City and Region accuracy to 17.78%, 40.57%

432

433

434

435

436

437

438

439

440

441

442

443

Table 3: The ablation results of Clue2Geo on Im2GPS3k (without Coordinate Refinement).

and 54.02%, respectively, indicating that structured cue modeling and multi-level guided reasoning provide valuable contextual constraints that stabilize and improve performance at medium to high granularities. Finally, removing CR leaves City and Region largely unaffected but sharply reduces Street accuracy to 15.45%, highlighting the retrieval module’s unique role in mitigating prediction variance, supplying reference coordinates aligned with real-world distributions, and boosting fine-grained stability and precision.

We found that post-coordinate refinement often acts as a “safety net” in the final results, masking the true contributions of other modules. To eliminate the stability compensation and smoothing effects introduced by coordinate refinement, we removed it, allowing the model’s multi-scale geolocation and reasoning capabilities to be directly evaluated in a “raw output” state. Table 3 presents the ablation results under this setting.

Without coordinate refinement, removing RC drops accuracy to 14.58% (Street), 40.44% (City), and 54.35% (Region), indicating that RC helps establish coarse spatial layouts and macro-level geographic semantics, thereby laying the foundation for subsequent fine-grained localization. In contrast, removing RL causes a sharp decline to 9.34% (Street) and 36.97% (City), showing that RL mainly supports fine-grained reasoning and multi-cue integration, greatly enhancing the model’s ability to recognize complex landmarks and local environments. The removal of OL has the most pronounced effect, reducing accuracy to 5.27% (Street) and 26.33% (City), which underscores OL as a key component for maintaining fine-grained performance. Without OL, the model relies primarily on coarse-grained information, causing fine-level metrics to nearly halve. Similarly, removing CM leads to noticeable drops across all metrics, falling to 13.61% (Street) and 36.87% (City). This demonstrates that CM not only provides essential supplementary information for fine-grained street-level localization but also acts as a stabilizing framework for large-scale reasoning.

These results indicate that Clue2Geo’s design is not a simple stacking of modules but a synergistic multi-modal and multi-stage system: the cluemap stabilizes multi-scale reasoning, coarse-grained tuning provides global spatial awareness, landmark-level tuning enhances fine-grained recognition, fine-grained optimization ensures precise direct prediction, and post-coordinate refinement smooths errors and improves robustness. Together, these modules enable the model to achieve breakthroughs in fine-grained geolocation while maintaining coarse-grained accuracy, demonstrating balanced, robust, and high-precision performance across multi-scale tasks.

5 CONCLUSION

In this study, we propose Clue2Geo, a global image geolocation framework that integrates LVLMs with structured geographic cues. Unlike previous approaches relying on single visual features or lacking explicit structural modeling, Clue2Geo systematically extracts cues and constructs a cluemap to capture their relationships and importance. By introducing local consistency and semantic coherence, it identifies the most representative cues and models their relationships, providing structured and interpretable inputs for geolocation. We further design a three-stage fine-tuning strategy, from city-level to landmark-level and optimization, to enhance the model’s multi-scale reasoning ability. In addition, a post-processing module based on RAG effectively mitigates prediction bias and further improves the stability and accuracy of fine-grained localization. Experimental results show that Clue2Geo achieves significant performance gains across multiple scales and scenarios, demonstrating superior generalization, interpretability, and robustness in cross-domain environments, and offering new directions for global image geolocation research and applications.

486 ETHICS STATEMENT
487488 We use publicly available street-view images from Mapillary to fine-tune large models for geoloca-
489 tion tasks. Although Mapillary has already blurred faces and license plates to protect privacy, private
490 residences remain visible in the images. All data usage complies with Mapillary’s CC BY-SA li-
491 cense, with proper attribution provided. Users should be aware of potential geographic or cultural
492 biases and avoid applications that could infringe on privacy or enable surveillance. Our resources
493 are intended solely for research purposes.
494495 REPRODUCIBILITY STATEMENT
496497 Due to space constraints in the main text, we are unable to provide detailed implementation details
498 of Clue2Geo. To ensure reproducibility, we provide the complete implementation details in the
499 appendix, including the cue extraction methods, prompts used for fine-tuning, the construction of
500 the cluemap, and the usage of the retrieval database.
501502 REFERENCES
503504 Josh Achiam, Steven Adler, Sandhini Agarwal, Lama Ahmad, Ilge Akkaya, Florencia Leoni Ale-
505 man, Diogo Almeida, Janko Altenschmidt, Sam Altman, Shyamal Anadkat, et al. Gpt-4 technical
506 report. *arXiv preprint arXiv:2303.08774*, 2023.507 Jinze Bai, Shuai Bai, Yunfei Chu, Zeyu Cui, Kai Dang, Xiaodong Deng, Yang Fan, Wenbin Ge,
508 Yu Han, Fei Huang, et al. Qwen technical report. *arXiv preprint arXiv:2309.16609*, 2023.
509510 Shuai Bai, Keqin Chen, Xuejing Liu, Jialin Wang, Wenbin Ge, Sibo Song, Kai Dang, Peng Wang,
511 Shijie Wang, Jun Tang, et al. Qwen2. 5-vl technical report. *arXiv preprint arXiv:2502.13923*,
512 2025.513 Bingyi Cao, Andre Araujo, and Jack Sim. Unifying deep local and global features for image search.
514 In *European conference on computer vision*, pp. 726–743. Springer, 2020.
515516 Brandon Clark, Alec Kerrigan, Parth Parag Kulkarni, Vicente Vivanco Cepeda, and Mubarak Shah.
517 Where we are and what we’re looking at: Query based worldwide image geo-localization using
518 hierarchies and scenes. In *Proceedings of the IEEE/CVF Conference on Computer Vision and*
519 *Pattern Recognition*, pp. 23182–23190, 2023.520 Nicolas Dufour, Vicky Kalogeiton, David Picard, and Loic Landrieu. Around the world in 80
521 timesteps: A generative approach to global visual geolocation. In *Proceedings of the Computer*
522 *Vision and Pattern Recognition Conference*, pp. 23016–23026, 2025.
523524 Mike Izbicki, Evangelos E Papalexakis, and Vassilis J Tsotras. Exploiting the earth’s spherical ge-
525 ometry to geolocate images. In *Joint European Conference on Machine Learning and Knowledge*
526 *Discovery in Databases*, pp. 3–19. Springer, 2019.527 Pengyue Jia, Jingtong Gao, Xiaopeng Li, Zixuan Wang, Yiyao Jin, and Xiangyu Zhao. Second place
528 overall solution for amazon kdd cup 2024. In *Amazon KDD Cup 2024 Workshop*, 2018.
529530 Pengyue Jia, Yiding Liu, Xiangyu Zhao, Xiaopeng Li, Changying Hao, Shuaiqiang Wang, and
531 Dawei Yin. Mill: Mutual verification with large language models for zero-shot query expansion.
532 *arXiv preprint arXiv:2310.19056*, 2023.533 Pengyue Jia, Yiding Liu, Xiaopeng Li, Xiangyu Zhao, Yuhao Wang, Yantong Du, Xiao Han, Xuetao
534 Wei, Shuaiqiang Wang, and Dawei Yin. G3: an effective and adaptive framework for worldwide
535 geolocalization using large multi-modality models. *Advances in Neural Information Processing*
536 *Systems*, 37:53198–53221, 2024.
537538 Seongwon Lee, Hongje Seong, Suhyeon Lee, and Euntai Kim. Correlation verification for image
539 retrieval. In *Proceedings of the IEEE/CVF conference on computer vision and pattern recognition*,
pp. 5374–5384, 2022.

540 Ling Li, Yu Ye, Bingchuan Jiang, and Wei Zeng. Georeasoner: Geo-localization with reasoning
 541 in street views using a large vision-language model. In *Forty-first International Conference on*
 542 *Machine Learning*, 2024.

543

544 Xiaopeng Li, Lixin Su, Pengyue Jia, Suqi Cheng, Junfeng Wang, Dawei Yin, and Xiangyu Zhao.
 545 Agent4ranking: Semantic robust ranking via personalized query rewriting using multi-agent llms.
 546 *ACM Transactions on Information Systems*, 2023.

547

548 Haotian Liu, Chunyuan Li, Qingyang Wu, and Yong Jae Lee. Visual instruction tuning. *Advances*
 549 *in neural information processing systems*, 36:34892–34916, 2023.

550

551 Liu Liu and Hongdong Li. Lending orientation to neural networks for cross-view geo-localization.
 552 In *Proceedings of the IEEE/CVF conference on computer vision and pattern recognition*, pp.
 553 5624–5633, 2019.

554

555 Eric Muller-Budack, Kader Pustu-Iren, and Ralph Ewerth. Geolocation estimation of photos using
 556 a hierarchical model and scene classification. In *Proceedings of the European conference on*
 557 *computer vision (ECCV)*, pp. 563–579, 2018.

558

559 Hyeonwoo Noh, Andre Araujo, Jack Sim, Tobias Weyand, and Bohyung Han. Large-scale image
 560 retrieval with attentive deep local features. In *Proceedings of the IEEE international conference*
 561 *on computer vision*, pp. 3456–3465, 2017.

562

563 Shraman Pramanick, Ewa M Nowara, Joshua Gleason, Carlos D Castillo, and Rama Chellappa.
 564 Where in the world is this image? transformer-based geo-localization in the wild. In *European*
 565 *Conference on Computer Vision*, pp. 196–215. Springer, 2022.

566

567 Shuofei Qiao, Yixin Ou, Ningyu Zhang, Xiang Chen, Yunzhi Yao, Shumin Deng, Chuanqi Tan, Fei
 568 Huang, and Huajun Chen. Reasoning with language model prompting: A survey. *arXiv preprint*
 569 *arXiv:2212.09597*, 2022.

570

571 Alec Radford, Jong Wook Kim, Chris Hallacy, Aditya Ramesh, Gabriel Goh, Sandhini Agarwal,
 572 Girish Sastry, Amanda Askell, Pamela Mishkin, Jack Clark, et al. Learning transferable visual
 573 models from natural language supervision. In *International conference on machine learning*, pp.
 574 8748–8763. PmLR, 2021.

575

576 Krishna Regmi and Mubarak Shah. Bridging the domain gap for ground-to-aerial image matching.
 577 In *Proceedings of the IEEE/CVF International Conference on Computer Vision*, pp. 470–479,
 578 2019.

579

580 Paul Hongsuck Seo, Tobias Weyand, Jack Sim, and Bohyung Han. Cplanet: Enhancing image ge-
 581 olocalization by combinatorial partitioning of maps. In *Proceedings of the European Conference*
 582 *on Computer Vision (ECCV)*, pp. 536–551, 2018.

583

584 Shihao Shao, Kaifeng Chen, Arjun Karpur, Qinghua Cui, André Araujo, and Bingyi Cao. Global
 585 features are all you need for image retrieval and reranking. In *Proceedings of the IEEE/CVF*
 586 *International Conference on Computer Vision*, pp. 11036–11046, 2023.

587

588 Yujiao Shi, Liu Liu, Xin Yu, and Hongdong Li. Spatial-aware feature aggregation for image based
 589 cross-view geo-localization. *Advances in Neural Information Processing Systems*, 32, 2019.

590

591 Yujiao Shi, Xin Yu, Dylan Campbell, and Hongdong Li. Where am i looking at? joint location and
 592 orientation estimation by cross-view matching. In *Proceedings of the IEEE/CVF Conference on*
 593 *Computer Vision and Pattern Recognition*, pp. 4064–4072, 2020.

594

595 Fuwen Tan, Jiangbo Yuan, and Vicente Ordonez. Instance-level image retrieval using reranking
 596 transformers. In *proceedings of the IEEE/CVF international conference on computer vision*, pp.
 597 12105–12115, 2021.

598

599 Aysim Toker, Qunjie Zhou, Maxim Maximov, and Laura Leal-Taixé. Coming down to earth:
 600 Satellite-to-street view synthesis for geo-localization. In *Proceedings of the IEEE/CVF Con-*
 601 *ference on Computer Vision and Pattern Recognition*, pp. 6488–6497, 2021.

594 Vicente Vivanco Cepeda, Gaurav Kumar Nayak, and Mubarak Shah. Geoclip: Clip-inspired align-
 595 ment between locations and images for effective worldwide geo-localization. *Advances in Neural*
 596 *Information Processing Systems*, 36:8690–8701, 2023.

597

598 Nam Vo, Nathan Jacobs, and James Hays. Revisiting im2gps in the deep learning era. In *Proceedings*
 599 *of the IEEE international conference on computer vision*, pp. 2621–2630, 2017.

600 Peng Wang, Shuai Bai, Sinan Tan, Shijie Wang, Zhihao Fan, Jinze Bai, Keqin Chen, Xuejing Liu,
 601 Jialin Wang, Wenbin Ge, et al. Qwen2-vl: Enhancing vision-language model’s perception of the
 602 world at any resolution. *arXiv preprint arXiv:2409.12191*, 2024.

603

604 Wenhui Wang, Zhe Chen, Xiaokang Chen, Jiannan Wu, Xizhou Zhu, Gang Zeng, Ping Luo, Tong
 605 Lu, Jie Zhou, Yu Qiao, et al. Visionllm: Large language model is also an open-ended decoder
 606 for vision-centric tasks. *Advances in Neural Information Processing Systems*, 36:61501–61513,
 607 2023.

608 Tobias Weyand, Ilya Kostrikov, and James Philbin. Planet-photo geolocation with convolutional
 609 neural networks. In *European conference on computer vision*, pp. 37–55. Springer, 2016.

610

611 Scott Workman, Richard Souvenir, and Nathan Jacobs. Wide-area image geolocalization with aerial
 612 reference imagery. In *Proceedings of the IEEE International Conference on Computer Vision*, pp.
 613 3961–3969, 2015.

614 Shukang Yin, Chaoyou Fu, Sirui Zhao, Ke Li, Xing Sun, Tong Xu, and Enhong Chen. A survey on
 615 multimodal large language models. *National Science Review*, 11(12):nwae403, 2024.

616

617 Wayne Xin Zhao, Kun Zhou, Junyi Li, Tianyi Tang, Xiaolei Wang, Yupeng Hou, Yingqian Min,
 618 Beichen Zhang, Junjie Zhang, Zican Dong, et al. A survey of large language models. *arXiv*
 619 *preprint arXiv:2303.18223*, 1(2), 2023.

620 Zhongliang Zhou, Jielu Zhang, Zihan Guan, Mengxuan Hu, Ni Lao, Lan Mu, Sheng Li, and
 621 Gengchen Mai. Img2loc: Revisiting image geolocalization using multi-modality foundation mod-
 622 els and image-based retrieval-augmented generation. In *Proceedings of the 47th international acm*
 623 *sigir conference on research and development in information retrieval*, pp. 2749–2754, 2024.

624

625 Sijie Zhu, Taojiaannan Yang, and Chen Chen. Vigor: Cross-view image geo-localization beyond one-
 626 to-one retrieval. In *Proceedings of the IEEE/CVF Conference on Computer Vision and Pattern*
 627 *Recognition*, pp. 3640–3649, 2021.

628

629 Sijie Zhu, Mubarak Shah, and Chen Chen. Transgeo: Transformer is all you need for cross-view
 630 image geo-localization. In *Proceedings of the IEEE/CVF Conference on Computer Vision and*
 631 *Pattern Recognition*, pp. 1162–1171, 2022.

632

633 A APPENDIX

634 A.1 EXPERIMENTAL DETAILS

636 A.1.1 CLUEMAP CONSTRUCTION

638 For the cue extraction component, we designed the following prompt, as shown in Figure 2.

639 For the construction of the cluemap, we used **CLIP-cn-vit-h-14** as the visual and text encoder for
 640 local consistency, and **text2vec-base-chinese** as the text encoder for semantic coherence. The
 641 final importance score was assigned a weight of **0.5**, meaning the importance was calculated as the
 642 average of local consistency and semantic coherence.

644 A.1.2 MULTI-SCALE LOCALIZATION FINE-TUNING

646 For the city-level reasoning fine-tuning, landmark-level reasoning fine-tuning, and landmark-level
 647 location optimization, we designed the JSON format. The example content is shown in the figure 3, 4
 and 5.

648 Extract and list all visually identifiable cues from the image that may be related to its geographic location:
 649
 650 1) Landmark buildings or distinctive structures — describe their detailed characteristics and quantify them
 651 when possible;
 652 2) Natural landscape features (e.g., mountains, coastlines, specific vegetation);
 653 3) Scene type (e.g., urban street view, rural field, indoor);
 654 4) Any recognizable text in the image (e.g., road signs, shop signs, billboards — attempt to transcribe the
 655 text content);
 656 5) Types or characteristics of vehicles (e.g., distinctive taxis or buses);
 657 6) Typical clothing or activities of people;
 658 7) Overall environmental atmosphere and style (e.g., weather, lighting).

659 The above types are for reference only — do not limit yourself to these categories. Each cue should be
 660 described in as much detail as possible.

661 Output format: (cue, detailed description of the cue)

662 Example:

663 (Tower structure, A tall tower with a complex metal framework, rectangular base tapering upwards with a
 664 pointed top, symmetrical geometric design resembling the Eiffel Tower)

665 Extract as many cues as possible — there is no upper limit, but provide at least five.

666 Even subtle cues that might aid geographic inference should be included.

667 Output only the cues; do not include control characters or any prediction of the geographic location.

668 Figure 2: Prompt for extracting cues

669 "**User**": "According to the content of the picture, please deduce which country the picture appears in. Please
 670 give the most likely answer and reasons, output in JSON format, e.g. {'country': '**city**': '**Reasons**'}.

672 "**Assitant**": {"country": "US", "city": "Chicago", "Reasons": "This map shows some of the even numbered US
 673 interstates that run east-west. The map also highlights that even numbered US interstate highway numbers
 674 gradually increase the further north you travel (I-10 is in the south of the US whilst I-90 in the north). Note'}

676 Figure 3: The example of city-level reasoning fine-tuning

677 A.1.3 POST-PROCESSING COORDINATE REFINEMENT

681 In the post-processing coordinate refinement stage, for each predicted image we retrieved the 15
 682 most similar and 15 least similar coordinates. Following the procedure described in (Jia et al.,
 683 2024), we used three separate prompts, each time providing 5, 10, or 15 of the similar and dissim-
 684 ilar reference coordinates respectively, and generated 1 predicted coordinate per prompt. We then
 685 merged these 3 predicted coordinates with the original predicted coordinate to form a set of candi-
 686 date coordinates. Finally, using the CLIP encoder described in (Jia et al., 2024), we encoded both
 687 the image and the candidate coordinates and selected the coordinate with the highest similarity score
 688 as the final prediction.

689 B THE USE OF LLMS

690 We employed LLMs to support our workflow throughout this study. Specifically, we leveraged GPT-
 691 4o to assist in debugging portions of the code, helping to identify errors and suggest corrections;
 692 and to refine and polish sections of the manuscript, improving clarity, sentence structure, and overall
 693 readability.

694
 695
 696
 697
 698
 699
 700
 701

702

703

704

705

706

707

708

709

710

711

712

713

714

715

716

717

718

719

720

721

722

723

724

725

726

727

728

729

730

731

732

733

734

735

736

737

738

739

740

741

742

743

744

745

746

747

748

749

750

751

752

753

754

755

"User": "Based on the content of the image, infer the country where the scene appears and provide the most likely answer. Then, follow these steps for multi-step reasoning using the extracted clues to identify the most probable city and its landmark:

1. Consider only the most important clue set 1, and determine a few candidate cities and landmarks it may point to.
2. Incorporate the second important clue set 2, and output the candidate cities and landmarks based on combined reasoning from sets 1 and 2.
3. Introduce the third clue set 3, integrate all three clue sets, and output the single city and landmark most likely.

For the predicted location, output the corresponding GPS coordinates.

Notes:

- If the city or landmark cannot be determined, fill in null.
- Coordinates must be in decimal degrees (DD) format, not degrees-minutes-seconds (DMS) or any other format, and retain at least four decimal places.
- If there is no city or landmark, return the center coordinates of the next higher-level region.

Input clues in order of importance:

1. Clue Set 1:

- Symmetrical composition: Four statues symmetrically distributed along a central axis, with equal spacing on both sides, forming a strict geometric layout.
- Giant stone sculptures: Four male heads carved into the mountain arranged east-west, from west to east: a white male with a wig, a bearded white male, a white male with a dome hat, and a black male with short hair, showing distinct racial features.
- Coniferous forest vegetation: Tall fir-like trees in the foreground, with conical crowns and straight trunks, approximately 3–5 meters high.

2. Clue Set 2:

- Historical commemorative style: Sculptures in classical realistic style, focusing on facial muscle details, characteristic of late 19th-century public art.

3. Clue Set 3:

- No man-made buildings: Besides the stone sculptures, no houses, roads, or human constructions, preserving the natural mountain shape.
- Overcast lighting: Sky covered with uniform gray clouds, no direct sunlight, soft mountain shadows, low contrast.
- Granite mountain: Hard gray-white rock with black spots, visible artificial carving marks, approximately 18 meters high and 24 meters wide.

"Assitant":

- 'country': 'United States', 'city': 'South Dakota', 'landmark': 'Mount Rushmore',
- 'lat': '43.8811', 'lon': '-103.4542',
- 'Reasons': 'Based on the provided visual clues, the location can be inferred as Mount Rushmore in South Dakota, USA: first, the four giant male heads are arranged east-west in a symmetrical composition carved on a granite mountain approximately 18 meters high and 24 meters wide, matching the distinctive features of the Rushmore monument; second, the figures from west to east are Washington (with a wig), Jefferson (bearded), Lincoln (with a dome hat), and Theodore Roosevelt (originally planned as a Native American figure but actually unfinished; the description incorrectly identifies the fourth as a Black male, yet the overall layout points to the four US presidents on Mount Rushmore); additionally, the sculptures are in late 19th-century classical realistic style, emphasizing facial muscle details, consistent with Mount Rushmore's carving style; furthermore, no man-made buildings are visible, the natural mountain shape is preserved, the vegetation consists of tall fir-like coniferous trees, and the lighting is overcast with low contrast, all matching the natural environment of the Black Hills in South Dakota, confirming the scene as Mount Rushmore.'

Figure 4: The example of landmark-level reasoning fine-tuning

756
757
758
759
760
761
762
763

764 "User": "Based on the content of the image, infer the country where the scene appears and provide the most likely
765 answer. Then, follow these steps for multi-step reasoning using the extracted clues to identify the most probable city
766 and its landmark:

- 767 1. Consider only the most important clue set 1, and determine a few candidate cities and landmarks it may point
768 to.
- 769 2. Incorporate the second important clue set 2, and output the candidate cities and landmarks based on
770 combined reasoning from sets 1 and 2.
- 771 3. Introduce the third clue set 3, integrate all three clue sets, and output the single city and landmark most likely.
772

773 For the predicted location, output the corresponding GPS coordinates.

774 **Notes:**

- 775 • If the city or landmark cannot be determined, fill in `null`.
- 776 • Coordinates must be in decimal degrees (DD) format, not degrees-minutes-seconds (DMS) or any other
777 format, and retain at least four decimal places.
- 778 • If there is no city or landmark, return the center coordinates of the next higher-level region.

781 **Input clues in order of importance:**

782 1. **Clue Set 1:**

- 783 • Traditional architecture: The buildings feature a typical East Asian style, with red pillars and gray tiled
784 roofs, decorated with exquisite painted patterns, and have a symmetrical and solemn structure.
- 785 • Scene type: An outdoor courtyard with a stone-paved ground, surrounded by traditional
786 buildings and modern signboards, clean and historically atmospheric.
- 787 • Signboard: A vertical black signboard on the left side of the courtyard with white text and patterns,
788 though the exact content is unclear.

789 2. **Clue Set 2:**

- 790 • Stone steps and platform: Several wide stone steps in the center of the square leading to a high
791 platform, with railings on both sides, designed simply and rustic.
- 792 • Human activity: Several people walking or standing on the open space in front of the building, wearing
793 modern casual clothes, seemingly visiting or sightseeing.

794 3. **Clue Set 3:**

- 795 • Red pillars: The building's supporting pillars are bright red, with smooth surfaces and stone bases at
796 the bottom, making them very striking.

797 "Assistant": "country": "South Korea", "city": "South Korea", "landmark": "1 street", "lat": "37.28178572", "lon": "127.0131513",
798

801 **Figure 5:** The example of landmark-level location optimizarion
802

803
804
805
806
807
808
809